

N. K. RAMAN¹, S. WALLACE², AND C. J. BRINKER^{1,3}. ¹Center for Micro-Engineered Ceramics, University of New Mexico, Albuquerque, NM 87131. ²Nanopore Corporation, 2501 Alamo Ave., SE, Albuquerque, NM 87106. ³Sandia National Laboratories, Advanced Materials Laboratory, 1001 University Blvd., SE, Albuquerque, NM 87106.

ABSTRACT

We have studied the different driving forces behind syneresis in MTES/TEOS gels by aging them in different H₂O/EtOH pore fluids. We show using shrinkage, density, contact angle, and N₂ sorption measurements, the influence of gel/solvent interactions on the microstructural evolution during drying. Competing effects of syneresis (that occurs during aging) and drying shrinkage resulted in the overall linear shrinkage of the organically modified gels to be constant at ~50%. Increasing the hydrophobicity of the gels caused the driving force for syneresis to change from primarily condensation reactions to a combination of condensation and solid/liquid interfacial energy. In addition the condensation driven shrinkage was observed to be irreversible, whereas the interfacial free energy driven shrinkage was observed to be partially reversible. Nitrogen sorption experiments show that xerogels with the same overall extent of shrinkage can have vastly different microstructures due to the effects of microphase separation.

INTRODUCTION

The extent of gel shrinkage during aging and drying from solvents such as water and ethanol is determined by: (1) condensation or reesterification reactions that strengthen or weaken the gel network, (2) solid/liquid interfacial free energy, (3) coarsening mechanisms that reduce the solid/liquid interfacial area and increase the network modulus, (4) microphase separation that increases the average pore size in gels, and (5) the competition between the capillary pressure exerted by the pore fluid that serves to compact the gel and the network modulus that resists compaction [1,2]. Several applications including gas separation membranes require both small pore sizes and high pore volumes. The organic template approach in which ligands are embedded in a dense inorganic matrix and selectively removed to create pores offers the ability to tailor pore volume independently of pore size [3]. In addition to their role as pore size-directing templates, organic ligands introduced as pendant groups (alkyltrialkoxysilanes, RTES) modify the network by reducing the functionality and therefore the mechanical stiffness of the network, and make the network more hydrophobic. The hydrophobicity of the gel governs the interactions between the gel and the pore fluid during aging and drying, and strongly influences both the tendency for phase separation and the magnitude of the drying stress. A better understanding of these issues would obviously help in the rational control of xerogel microstructures.

Aging

Syneresis is defined as the spontaneous shrinkage of the gel during aging due to the expulsion of solvent from its pores [1,4]. Syneresis is known to occur by different mechanisms in inorganic or organic gels. Syneresis in inorganic gels is attributed mainly to continuing condensation reactions and coarsening, and the syneresis rate is minimized at isoelectric point of silica where the condensation rate is minimized [1]. Syneresis driven by condensation reactions is generally observed to be irreversible. For example, irreversible syneresis was observed in pure TEOS gels to increase from about 1% in pure ethanol to about 16% in pure water [4]. Coarsening occurs due to differences in the solubility between surfaces having different radii of curvature [1]. During the coarsening process, smaller particles dissolve and precipitate on larger particles or on necks between particles that have negative radii, hence, lower solubility. Coarsening does not produce shrinkage because the centers of the particle do not move toward one another, but reduces the interfacial area and increases the strength of the network [1]. Because of the low solubility of silica under acidic conditions, significant coarsening is not expected to occur in acid-catalyzed gels.

Syneresis could also result from the gel network attempting to reduce its huge solid/liquid interfacial area. Scherer [1,4] has derived an expression for the linear strain rate that occurs during the interfacial free energy driven syneresis. However, the shrinkage rate predicted by the equation was too fast, and based on syneresis studies on acid-catalyzed TEOS gels, it was concluded that

DISTRIBUTION OF THIS DOCUMENT IS UNLIMITED

MASTER

FIVE
JUL 02 1996
OSTI

the structural rearrangements needed to cause this shrinkage does not occur in inorganic gels. Syneresis driven by interfacial free energies is atleast partially reversible. For example, organic gels are known to undergo reversible syneresis [5] with changing temperature, ionic strength etc. The shrinkage and the microstructural changes that occur during syneresis greatly impact the shrinkage and microstructural evolution during drying.

Drying

Syneresis is a self-limiting process. It slows down due to the decreasing network permeability and the stiffness of the gels which increases with shrinkage as a power law [1]:

$$K_p = K_0 (V_0/V)^m \quad (1)$$

where K_0 and K_p are the initial and instantaneous bulk modulus of the gel, V_0 is the shrunken volume, and $m = 3.0-3.8$. To further densify the gel it is necessary to remove the pore fluid by drying. During the initial stages of drying, capillary tension develops in the pore fluid. The gel network, in response, shrinks to support this tension. Drying shrinkage stops when the increasing gel stiffness balances this tension. This balancing point is referred to as the critical point because it establishes the final (dried) pore volume and pore size. The strain at the critical point, ϵ , is given by [1]:

$$\epsilon = \{(1-\phi_s)/K_p\} P_c \quad (2)$$

where ϕ_s is the volume fraction of solids and P_c is the maximum capillary stress at the critical point. During drying, if gelation precedes drying and K_0 is low (as in organically modified gels), the network may collapse sufficiently creating pores that are too small to empty at the relevant P/P_0 , so P_c is given by a form of the Kelvin-Laplace equation,

$$P_c = (R_p T/V_m) \ln(P/P_0) \quad (3)$$

where, R is the ideal gas constant, T is the temperature, V_m is the molar volume of the pore fluid, and P_0 is the saturation pressure of the pore fluid. Because K_p increases due to both syneresis and drying shrinkage, the extent of drying strain (eq. 2) will vary approximately inversely with the extent of syneresis shrinkage.

For organically modified systems in general, the RTES/TEOS ratio has several effects on syneresis: (1) organic ligands reduce the connectivity of the network and thus its initial modulus K_0 , (2) introduction of organic ligands causes the gel network to become progressively hydrophobic, and (3) organic ligands inhibit condensation reactions due to steric and solvation effects. The pore fluid water concentration has two related effects: (1) water is generally observed to promote condensation reactions, and (2) increased water concentration causes the solvent to become more polar reducing the solvent quality for hydrophobic polymers.

In this paper we report on the different driving forces behind syneresis in MTES/TEOS gels aged in different $H_2O/EtOH$ pore fluids, and show using shrinkage, density, contact angle, and N_2 sorption measurements, the influence of gel/solvent interactions on the microstructural evolution during drying.

EXPERIMENTAL PROCEDURE

Sol and Bulk Gel Preparation

Sols were prepared by co-polymerization of methyltriethoxysilane (MTES) and TEOS using a two-step acid-catalyzed procedure, referred to as the A2 process [3]. The MTES/TEOS mole ratio was varied by introducing MTES as a percentage of total silicon in the sol. Xerogel (dry gel) bulk samples for shrinkage measurements were cast in cylindrical molds (length 90 mm, diameter 5 mm), sealed, gelled at 50°C and aged for 24-48 hr. The gel rods were then inserted into 22 mm x 175 mm glass tubes for pore fluid exchange and drying. The original pore fluid was replaced by immersing gels in $H_2O/EtOH$ mixtures in a series of six steps. Seven pore fluid compositions between 0 and 100 vol% $H_2O/EtOH$ were investigated. The change in length of the gels was measured during syneresis and drying at 50°C. The gel rods were subsequently dried in air at 150°C for 8 hr with a heating and cooling rate of 0.1°C/min prior to further characterization.

Bulk and Skeletal Density Measurements

Samples for bulk density measurements were prepared by polishing 15-20 mm cylindrical gel rods to a smooth finish using a Carbimet® 600 Grit Silicon Carbide grinding paper (Buehler, Lake

Bluff, IL). The weight of the gel rods measured at 150°C was used in the bulk density calculation to avoid errors due to water condensation in the pores. The length and diameter of the samples were measured using a MAX-CAL digital vernier caliper (Cole-Parmer, Vernon Hills, IL) with an accuracy of ± 0.03 mm. An average of three to four measurements was used to calculate the bulk densities. Gel samples for skeletal density measurements were prepared by grinding the gel rods into fine powder using a mortar and pestle. An Accupyc 1330 Helium Pycnometer (Micromeritics, Norcross, GA) was used to measure skeletal densities after outgassing at 150°C for 12 hr. in ambient air. An equilibration rate of 0.01 psig/min was used for the density measurements. An average of 10 measurements with a standard deviation of ± 0.005 g/cc was used to calculate the skeletal densities.

Contact Angle Measurements

A VCA-2000 (AST, Bellerica, MA) sessile drop system with a video monitor and a tilting sample stage was used for contact angle measurements. The measurements were made on corresponding thin films prepared with identical compositions and dried at 150°C for 0.5 hr. Advancing contact angles were measured by adding liquids with a syringe. The image of the liquid drop was captured within 2 sec to avoid errors due to its reaction with the film surface. The measurements were performed in a closed environment that was shielded from dust and saturated with the solvent used to make the measurements. An average of six readings with an error of $\pm 3^\circ$ was used to calculate the contact angles. The polar ($\sim\gamma_p$) and dispersive ($\sim\gamma_d$) components of the interfacial free energies were calculated using the Owens-Wendt geometric mean method [6]. Contact angles of deionized water and 200 proof ethanol were used in the calculations.

Microstructural Characterization

An ASAP 2000 (Micromeritics, Norcross, GA) instrument was used to measure N_2 sorption isotherms of the bulk xerogels after outgassing at 150°C for 12 hr. at 0.01 torr. The apparent surface area (m^2/g) was calculated from the BET equation [7] using N_2 molecular cross sectional area = 0.162 nm² and the linear region between $0.05 < P/P_0 < 0.20$ that gave a least square correlation coefficient $R^2 > 0.9999$ for at least 4 adsorption points. The pore volume (cm^3/g) was calculated from the high P/P_0 portion of the isotherm where the volume of N_2 adsorbed was constant.

RESULTS AND DISCUSSIONS

Shrinkage results presented in Fig. 1(a) for MTES/TEOS gels as a function of increasing MTES and water concentration demonstrate the interplay of MTES/TEOS ratio and pore fluid water concentration on syneresis. At constant MTES/TEOS ratios, all the gels exhibited progressively higher syneresis with increasing pore fluid water concentration. For example, syneresis of the 55 mol% MTES/TEOS gels increased from about -1.5% in pure ethanol to about 25% in pure water. Increasing the MTES/TEOS ratio from 0 to 55 mol% caused the shrinkage to increase in pure water from 22% to 29%, while in pure ethanol it caused $\sim 1.5\%$ expansion. About 16% of syneresis was reversible for the 55 mol% MTES/TEOS gels aged in water.

The linear shrinkage of MTES/TEOS gels during drying is shown in Fig. 1(b) as a function of MTES/TEOS ratio and pore fluid water concentration. The linear shrinkage of the gels during drying exhibited an opposite trend compared to syneresis, consistent with the physical and chemical changes that occurred during syneresis. For example, shrinkage of the 55 mol% MTES/TEOS gels decreased from $\sim 50\%$ when dried from pure ethanol to $\sim 20\%$ when dried from pure water. However the overall shrinkage of the gels (including syneresis and drying) remained constant at $\sim 50\%$ (see Fig. 1(c)).

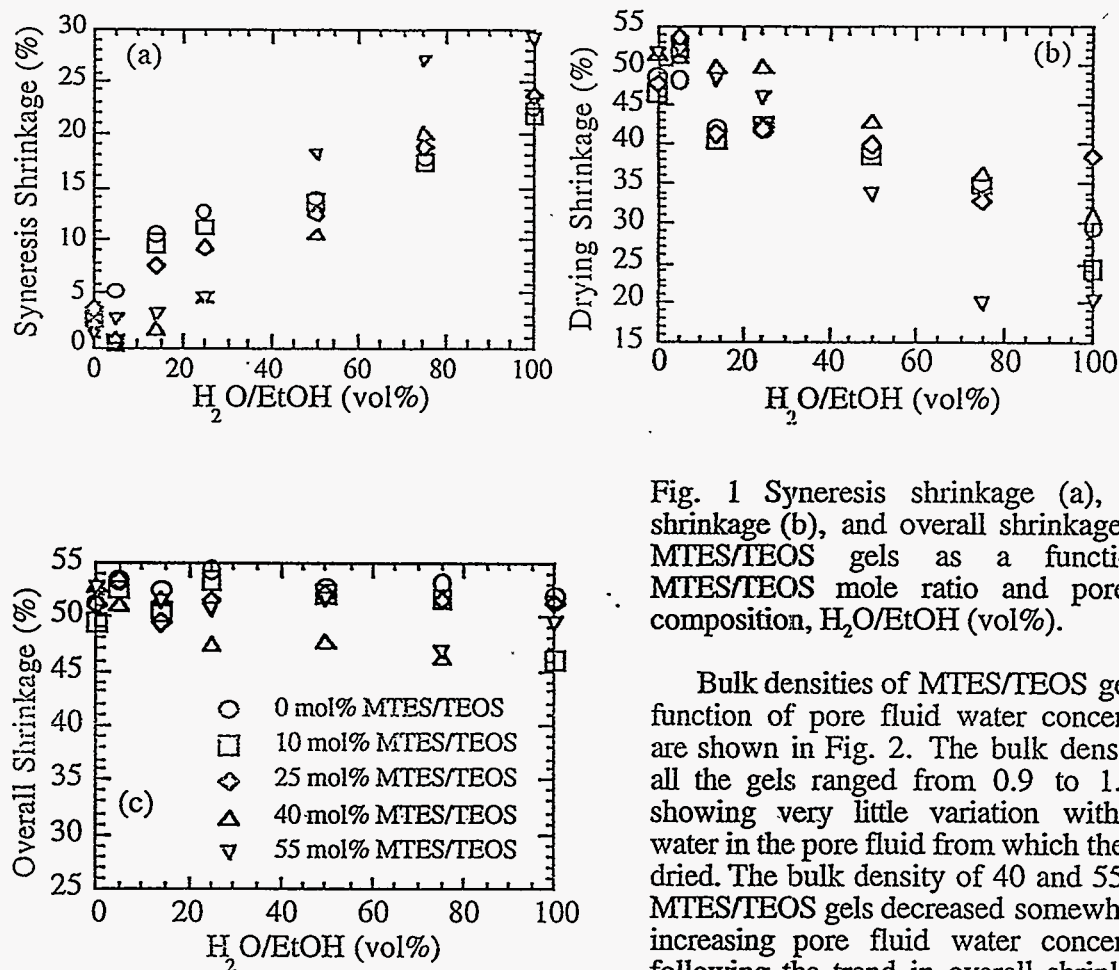


Fig. 1 Syneresis shrinkage (a), drying shrinkage (b), and overall shrinkage (c) of MTES/TEOS gels as a function of MTES/TEOS mole ratio and pore fluid composition, H₂O/EtOH (vol%).

Bulk densities of MTES/TEOS gels as a function of pore fluid water concentration are shown in Fig. 2. The bulk densities of all the gels ranged from 0.9 to 1.1 g/cc showing very little variation with vol% water in the pore fluid from which they were dried. The bulk density of 40 and 55 mol% MTES/TEOS gels decreased somewhat with increasing pore fluid water concentration following the trend in overall shrinkage of these gels. Skeletal densities of

MTES/TEOS xerogels as a function of pore fluid water concentration are plotted in Fig. 3. The skeletal density of 0 mol% MTES/TEOS gels increased from 1.7 g/cc to 2.185 g/cc as the water concentration in the pore fluid increased from 0 to 100 vol%. However, as the MTES content increased the variation (increase) in skeletal density with vol% water progressively decreased until at 55 mol% MTES/TEOS there was almost no variation in skeletal density. These results imply that with increasing MTES/TEOS ratios the driving force behind syneresis changes from condensation reactions which should result in an increase in skeletal density to a combination of condensation and interfacial free energies. This is consistent with the observation that with increasing MTES/TEOS mole ratios the syneresis shrinkage in 100% water became progressively more reversible.

Advancing contact angles for various EtOH/water mixtures are plotted in Fig. 3, as a function of MTES/TEOS mole ratios. As seen in Fig. 3 all the films exhibited a zero advancing contact angle for pure ethanol. The contact angles for the films increased with increasing H₂O/EtOH ratios with the 55 mol% MTES/TEOS showing the highest water contact angles (~80°). γ_s was very similar for all the samples at about 10 dynes/cm whereas γ_p decreased from about 49 dynes/cm for the 0 mol% MTES films to about 20 dyne/cm for the 55 mol% MTES film. The decrease in γ_p with

increasing MTES content is consistent with shrinkage and contact angle

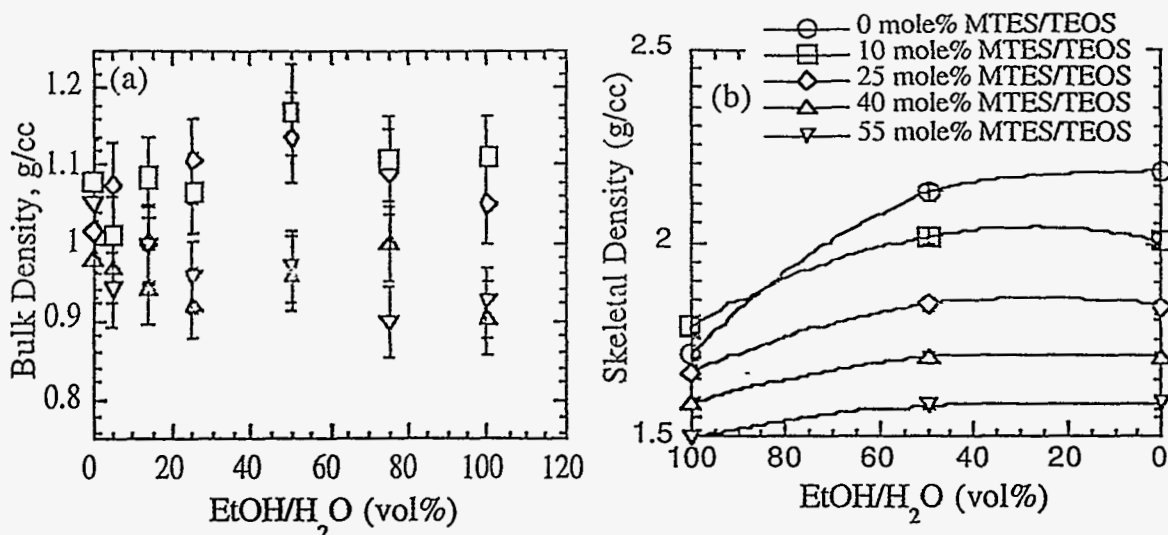


Fig. 2 Bulk density (a), and skeletal density (b) of MTES/TEOS gels as a function of pore fluid water concentration. The line is a visual guide.

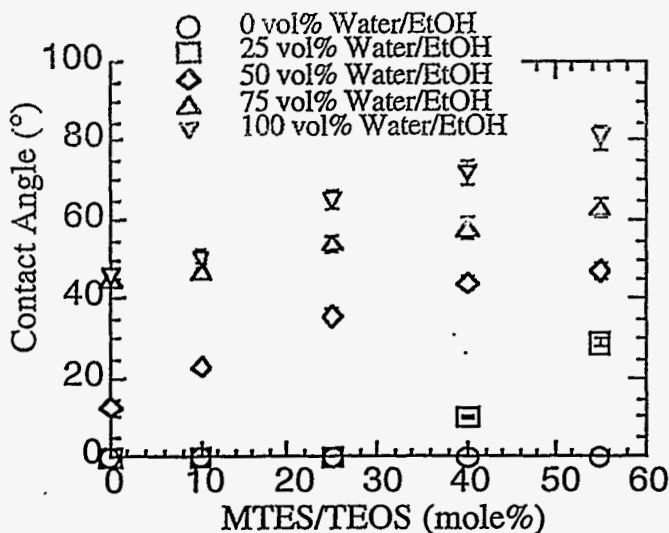


Fig. 3 Advancing contact angles of MTES/TEOS films as a function of MTES/TEOS mole ratio.

measurements which show the xerogels becoming increasingly hydrophobic. The total interfacial free energy of about 30 dynes/cm calculated for the 55 mol% MTES film is higher compared to a closed packed surface of methyl groups (21 dynes/cm [8]) indicating the presence of low levels of silanol groups in these films.

The effect of polymer/solvent interactions on xerogel microstructures is dramatically illustrated by the N_2 sorption isotherms shown in Fig. 4 for 55 mol% MTES/TEOS gels dried from EtOH, 50 vol% H_2O /EtOH and H_2O . Despite the fact that these gels exhibited about the same overall extent of drying shrinkage (Fig. 1(c)) they have

considerably different microstructures. The isotherm of the gel dried from pure ethanol is of Type I, characteristic of microporous materials. In addition, for a 5 sec equilibration interval, the adsorption and desorption branch of the isotherm did not converge due to the slow kinetics of adsorption and desorption in the very small pores [9]. On increasing the pore fluid water concentration from 0 to 50 to 100, vol%, the isotherms change from Type I to Type IV that is characteristic of mesoporous materials, showing a net increase in the average pore size of the gels. The increase in average pore size is consistent with microphase separation similar to that illustrated in reference [1].

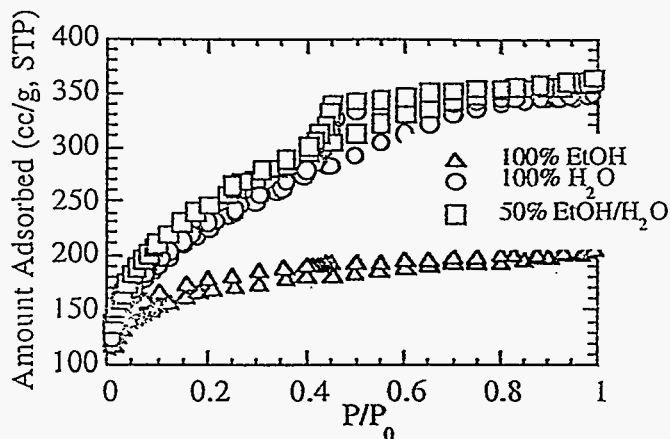


Fig. 4 Nitrogen sorption isotherms of 55 mol% MTES/TEOS xerogels versus pore fluid composition.

CONCLUSIONS

Syneresis in organic-inorganic gels results from both condensation and gel/solvent interactions and is sensitive to the organic/inorganic ratio and the pore fluid composition. The overall extent of shrinkage of MTES/TEOS gels dried from H₂O/EtOH compositions was constant at ~50%. With increasing hydrophobicity the driving force for syneresis changed from primarily condensation to a combination of condensation and interfacial free energies.

For the same overall extent of shrinkage, the increase in average pore size with increasing pore fluid water concentration was attributed to microphase separation.

ACKNOWLEDGMENTS

Portions of this work were supported by the Electric Power research Institute, the National Science Foundation (CTS 9101658), the Gas Research Institute, and the Department of Energy - Morgantown Energy Technology Center. One author (NKR) wishes to acknowledge the University of New Mexico for the award of RPT grant to attend this conference. In addition, we are grateful for H. Naraghi of University of New Mexico for the shrinkage Measurements. Sandia National Laboratories is a U.S. Department of Energy facility operated under Contract No. DE-AC04-94AL85000.

REFERENCES

- 1) C. J. Brinker and G. W. Scherer, *Sol-Gel Science* (Academic Press, New York, 1990).
- 2) W. G. Fahrenholtz and D. M. Smith, *Mat. Res. Soc. Symp. Proc. Vol. 271, 1992, 705-710*.
- 3) N. K. Raman and C. J. Brinker, *J. Memb. Sci.* 1995, 105, 273.
- 4) G. W. Scherer, *Mat. Res. Soc. Symp. Proc. Vol. 121, 1988, 179-197*.
- 5) T. Tanaka, *Sci. Amer.* 1981, 244, 124.
- 6) Allan F. M. Barton, *CRC Handbook of Solubility Parameters and Other Cohesive Parameters*, chapter 8, pages 159-161 and 430-432 (CRC Press, Boca Raton, Florida, 1983).
- 7) Stephen Wallace, C. Jeffrey Brinker, and Douglas M. Smith, *Mat. Res. Soc. Symp. Proc. vol. 371; 1995, 241-246*.
- 8) M. J. Owen, *Silicon-Based Polymer Science: A Comprehensive Resource*, 1990 Chapter 40, 705-739.
- 9) Y. Plevaya, J. Samuel, M. Ottolenghi, and D. Avnir, *J. Sol-Gel Sci. Tech.*, 1995, 5, 65.